2009 IEEE International Conference on Robotics and Automation
Kobe International Conference Center
Kobe, Japan, May 12-17, 2009

Modeling and Control of a Pair of Robot Fingers with Saddle Joint under Orderless Actuations

Morio Yoshida, Suguru Arimoto, and Kenji Tahara

***Abstract*— A new robot hand dynamics model with rolling constraints and with a saddle joint at one finger is proposed, where two saddle-joint actuations are considered to be orderless. Spinning motion around the opposition axis connecting two center points of each finger-tip contact area with an object is faithfully treated, and a viscosity model for damping rotational motion of the object is proposed. A class of control signals without referring to object kinematics or using external sensing is proposed. Finally, numerical simulation results show the stability of motion of the overall closed-loop dynamics supplied with the proposed control input.**

I. Introduction

The whole stimuli to the human brain, which arise from making and using tools by hands, have accelerated the evolutionary speed of the human brain. The primatologist Napier [1] claims that most of important movements of the hands are based upon finger-thumb opposition shown in Fig.1, that has contributed to the progress of humanity. Despite such a profound proposition, there is a dearth of robotic researches paying much attention to consideration of control functions of multi-fingered hands.

For the sake of raveling mysteries of the human hand and realizing its dexterous movements, many robotic researchers devote a lot of their elaborate efforts to the research of robot hands [2] [3] [4]. However, most of the researchers were attracted by kinematics and planning of motions realizing force/torque closure for stable grasp by robot fingers in a static sense. On the other hand, rolling geometry between two arbitrarily-shaped objects is rigorously discussed [5] [6]. However, all the researches have remained in a kinematic or semi-dynamic meaning. In the field of multibody dynamics [7], many models with constraints in 3-D space are presented without modeling physically faithful interaction between a robot finger and an object surface through 3-D rolling. An explicit 3-D dynamical pinching model with rolling constraints between a finger end and an object surface has been missing.

Around the year of 2000, Arimoto *et al.* first showed that 2-D object pinching is realized by using a pair of robot fingers with hemispherical ends, succeeding at embedding rolling constraints into the overall fingers-object dynamics [8] [9]. The degrees-of-freedom redundancy problem of the overall fingers-object dynamics for desired tasks is overcome by proposing a stability concept called "Stability on a

This work was partially supported by Japan Society for the Promotion of Science (JSPS), Grant-in-Aid for Scientific Research (B) (20360117).

M. Yoshida, S. Arimoto, and K. Tahara are with the RIKEN-TRI-Collaboration Center for Human-Interactive Robot Research, RIKEN, Nagoya, Aichi, 463-0003, Japan yoshida@nagoya.riken.jp

S. Arimoto is with the Department of Robotics, Ritsumeikan University, Kusatsu, Shiga, 525-8577, Japan arimoto@fc.ritsumei.ac.jp

K. Tahara is with the Organization for the Promotion of Advanced Research, Kyushu University, Fukuoka, 819-0395, Japan tahara@ieee.org

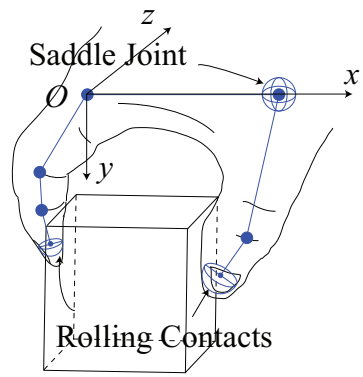

Fig. 1. Human pinch motion based on fingers-thumb opposition

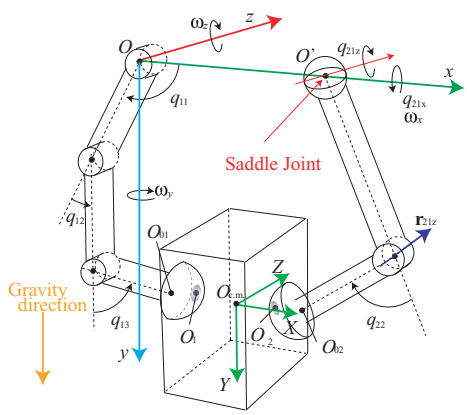

Fig. 2. Two robot fingers with soft tips pinching an object with parallel flat surfaces under gravity

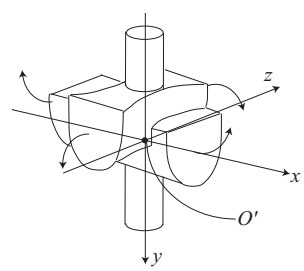

Fig. 3. Modeling of a saddle joint in human thumb [5]

manifold". In the year of 2006 [10], modeling of motion of pinching an object was extended from two-dimensional to three-dimensional pinching. In the modeling of pinching it is assumed that spinning motion of the object around the opposition axis connecting two contact points between the left or right finger end and the object surface has ceased and will not arise any more due to dry friction and micro-deformations near the two contact points. This assumption leads to a five-variables model of the object dynamics. In the year of 2008 [11] [12] [13], instead of this assumption, the modeling problem was posed as a more faithful model considering that spinning motion of the object is possible to arise but viscosity friction is exerted on x axis in the frame coordinates $O-xyz$ (see Figure 2), which means the overall fingers-object dynamics as a full variables model is derived. Furthermore, in the previous paper [12], two saddle-joint motors of the robot finger are actuated in sequence. However, the saddle joint of the human thumb must be actuated around the two axes respectively without making any order [14] (see Figure 3).

In this paper, we propose a saddle joint model with the orderless relation like the human thumb, and a robot hand model with the saddle joint through taking account of rolling constraints that are Pfaffian. A pair of robot fingers with hemispherical tips made from soft material is treated under the gravity effect. Simple control signals based on the opposability without using object kinematics or external sensing are shown, which are the same as the previously-proposed control signals [11] [12] [13]. Finally, for the sake of confirmation of the stability analysis, we carry out numerical simulations based on the proposed model of object-fingers dynamics and control signals.

II. Geometry of Robot Finger with Orderless Actuations

Since the first joint J_{21} of the robot finger shown in Fig.4 has orderless saddle-joint actuations, the Denavit-Hartenberg Notation is not applied to derive a geometrical relation of robot kinematics. In this section, a kinematic geometry of the robot finger with orderless actuations, the structure of which is similar to a saddle-joint model of the human thumb [14](see Figure 3), is derived. The coordinate system shown Fig.4 is right-handed. The first joint with center O' depicted in Fig.3 is a saddle joint exerted by two actuators, one of which rotates around x-axis and another around z- axis, $\dot{q}_{21x}$ denotes the angular velocity around x-axis and $\dot{q}_{21z}$ around z-axis respectively, where $\dot{\boldsymbol{q}}_{21} = (\dot{q}_{21x}, 0, \dot{q}_{21z})^{\mathrm{T}}$ denotes the rotational vector of the first link with the saddle joint in terms of frame coordinates $O' - xyz$ (see Figure 4). We set the Cartesian coordinates $O_{\mathrm{c.m.}21} - X_{21}Y_{21}Z_{21}$ fixed at the first link frame of the robot hand, and denote three orthogonal unit vectors at the first link frame in each corresponding direction X_{21},Y_{21}, and Z_{21} by $\boldsymbol{r}_{X21} = (r_{Xx21}, r_{Xy21}, r_{Xz21})^{\mathrm{T}}$, $\boldsymbol{r}_{Y21} = (r_{Yx21}, r_{Yy21}, r_{Yz21})^{\mathrm{T}}$, and $\boldsymbol{r}_{Z21} = (r_{Zx21}, r_{Zy21}, r_{Zz21})^{\mathrm{T}}$ as shown in Fig.4. We derive the mass center $O_{c.m.21}$ of the right robot finger by $\boldsymbol{x}_{m21} = (x_{m21}, y_{m21}, z_{m21})^{\mathrm{T}} = s_{21}\boldsymbol{r}_{Y21} + (L, 0, 0)^{\mathrm{T}}$ based

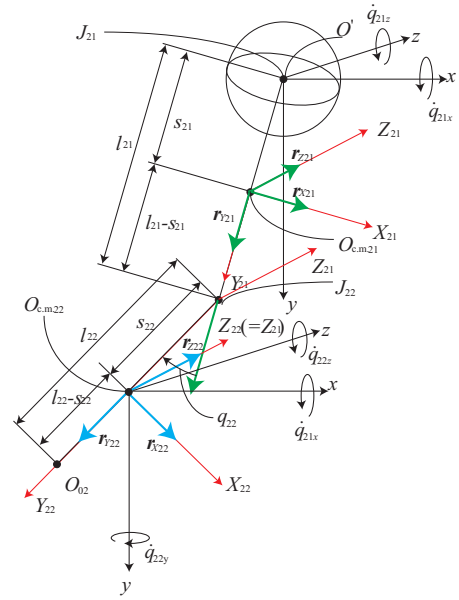

Fig. 4. Modeling of the right robot finger with a saddle joint which has orderless actuations

on the frame coordinates $O - xyz$ (see Figure 2). It is well known that the 3×3 rotation matrix

$$R_{21}(t) = (\boldsymbol{r}_{X21}, \boldsymbol{r}_{Y21}, \boldsymbol{r}_{Z21}) \in SO(3) \tag{1}$$

which is subject to the first-order differential equation representing infinitesimal rotation as follows:

$$\frac{\mathrm{d}}{\mathrm{d}t} R_{21}(t) = R_{21}(t)\Omega_{21}(t) \tag{2}$$

where

$$\Omega_{21}(t) = \begin{pmatrix} 0 & -\dot{q}_{21z} & 0 \\ \dot{q}_{21z} & 0 & -\dot{q}_{21x} \\ 0 & \dot{q}_{21x} & 0 \end{pmatrix} \tag{3}$$

The equations expressing the mass center $O_{\mathrm{c.m.}22}$ of the second link are derived by considering the relationship between the first link's posture and the angle q_{22} which rotates around Z_{21} as follows:

$$\boldsymbol{r}_{X22} = \cos q_{22}\boldsymbol{r}_{X21} + \sin q_{22}\boldsymbol{r}_{Y21} \tag{4}$$

$$\boldsymbol{r}_{Y22} = -\sin q_{22}\boldsymbol{r}_{X21} + \cos q_{22}\boldsymbol{r}_{Y21} \tag{5}$$

$$\boldsymbol{r}_{Z22} = \boldsymbol{r}_{Z21} \tag{6}$$

The angular velocity $\dot{\boldsymbol{q}}_{22} = (\dot{q}_{22x}, \dot{q}_{22y}, \dot{q}_{22z})^{\mathrm{T}}$ of the second link, which rotates around Z_{21}, can be represented by $\dot{\boldsymbol{q}}_{22} = \dot{q}_{22}\boldsymbol{r}_{Z21} + q_{22}\dot{\boldsymbol{r}}_{Z21}$. Therefore the mass center $O_{c.m.22}$ defined by $\boldsymbol{x}_{m22} = (x_{m22}, y_{m22}, z_{m22})^{\mathrm{T}}$ can be represented by $\boldsymbol{x}_{m22} = l_{21}\boldsymbol{r}_{Y21} + s_{22}\boldsymbol{r}_{Y22}$.

III. Dynamics

The model of pinching a rigid object with parallel flat surfaces by two robot fingers with 3 DOFs and 3 DOFs is schematically shown in Fig.2. The left finger (finger $i = 1$) is planar with three actuators rotational around z-axis. The

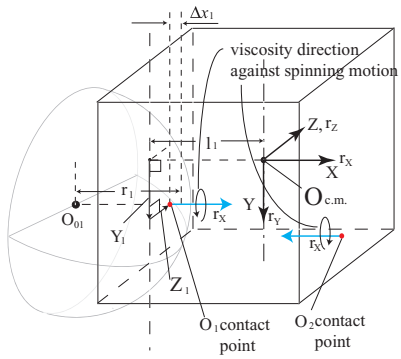

Fig. 5. r_X, r_Y, and r_Z vectors represent rotational movement of an object. Viscosity works around r_X vector at a contact point between a finger tip and an object surface

vector $\boldsymbol{q}_{11} = (q_{11}, q_{12}, q_{13})^{\mathrm{T}}$ denotes the joint angles of the left hand side finger. In the previous paper [10], it is also assumed that spinning around the opposition axis is possible to arise but viscosity damps rotational motion of the object around x-axis, that is, about ω_x, where $\boldsymbol{\omega} = (\omega_x, \omega_y, \omega_z)^{\mathrm{T}}$ denotes the vector of rigid body rotation in terms of frame coordinates O-xyz (see Figure 2). This viscosity model is effective but rough in a physical sense. Instead of it, we introduce a more faithful viscosity model which is exerted on rotational motion of the object around the $\boldsymbol{r}_X$ vector at two contact points between the left or right finger tip and the object surface as shown in Fig.5.

At the same time, we introduce the cartesian coordinates $O_{c.m.}$-XYZ fixed at the object frame and denote the three orthogonal unit vectors at the object frame in each corresponding direction X, Y, and Z by $\boldsymbol{r}_X = (r_{Xx}, r_{Xy}, r_{Xz})^{\mathrm{T}}$, $\boldsymbol{r}_Y = (r_{Yx}, r_{Yy}, r_{Yz})^{\mathrm{T}}$, and $\boldsymbol{r}_Z = (r_{Zx}, r_{Zy}, r_{Zz})^{\mathrm{T}}$ as shown in Fig.2. Next, let us denote the cartesian coordinates of the object mass center $O_{c.m.}$ by $\boldsymbol{x} = (x, y, z)^{\mathrm{T}}$ based on the frame coordinates O-xyz and note that three mutually orthogonal unit vectors fixed at the object frame may rotate dependently on the angular velocity vector $\boldsymbol{\omega}$ of body rotation. Then, it is well known that the 3×3 rotation matrix

$$R(t) = (\boldsymbol{r}_X, \boldsymbol{r}_Y, \boldsymbol{r}_Z) \in SO(3) \tag{7}$$

is subject to the first-order differential equation

$$\frac{\mathrm{d}}{\mathrm{d}t} R(t) = R(t)\Omega(t) \tag{8}$$

where

$$\Omega(t) = \begin{pmatrix} 0 & -\omega_z & \omega_y \\ \omega_z & 0 & -\omega_x \\ -\omega_y & \omega_x & 0 \end{pmatrix} \tag{9}$$

Next, denote the position of the center of each hemispherical finger-end by $\boldsymbol{x}_{0i} = (x_{0i}, y_{0i}, z_{0i})^{\mathrm{T}}$. Then, it is possible to notice that (see Fig.5)

$$\boldsymbol{x}_i = \boldsymbol{x}_{0i} - (-1)^i (r_i - \Delta x_i) \boldsymbol{r}_X \tag{10}$$

$$\boldsymbol{x} = \boldsymbol{x}_{0i} - (-1)^i (r_i - \Delta x_i + l_i) \boldsymbol{r}_X - Y_i \boldsymbol{r}_Y - Z_i \boldsymbol{r}_Z \tag{11}$$

Since each contact point O_i can be expressed by the coordinates $((-1)^i l_i, Y_i, Z_i)$ based on the object frame $O_{c.m.}$-XYZ, taking an inner product between Equation (11) and $\boldsymbol{r}_Y$ gives rise to

$$Y_i = (\boldsymbol{x}_{0i} - \boldsymbol{x})^{\mathrm{T}} \boldsymbol{r}_Y, \ i = 1, 2 \tag{12}$$

Similarly, it follows that

$$Z_i = (\boldsymbol{x}_{0i} - \boldsymbol{x})^{\mathrm{T}} \boldsymbol{r}_Z, \ i = 1, 2 \tag{13}$$

A rolling constraint between one finger-end and its contacted object surface can be expressed by the equality of two contact point velocities expressed on either of finger-end spheres and its corresponding tangent plane (that is coincident with one of object flat surfaces) as follows [10]:

$$\begin{cases} (r_1 - \Delta x_1) \{\omega_z - r_{Zz}(\dot{q}_{11} + \dot{q}_{12} + \dot{q}_{13})\} = \dot{Y}_1 \\ (r_1 - \Delta x_1) \{-\omega_y + r_{Yz}(\dot{q}_{11} + \dot{q}_{12} + \dot{q}_{13})\} = \dot{Z}_1 \end{cases} \tag{14}$$

$$\begin{cases} (r_2 - \Delta x_2) \{-\omega_z + r_{Zz}\dot{q}_{21z} + r_{Zx}\dot{q}_{21x} + \boldsymbol{r}_{Z21}^{\mathrm{T}} \boldsymbol{r}_Z \dot{q}_{22}\} = \dot{Y}_2 \\ (r_2 - \Delta x_2) \{\omega_y - r_{Yz}\dot{q}_{21z} - r_{Yx}\dot{q}_{21x} - \boldsymbol{r}_{Z21}^{\mathrm{T}} \boldsymbol{r}_Y \dot{q}_{22}\} = \dot{Z}_2 \end{cases} \tag{15}$$

The rolling constraint conditions expressed through Equations (14) and (15) are non-holonomic but linear and homogeneous with respect to velocity variables. Hence, Equations (14) and (15) can be treated as Pfaffian constraints [2] that can be expressed with accompaning Lagrange's multipliers $\{\lambda_{Y1}, \lambda_{Z1}\}$ for Equation (14), and $\{\lambda_{Y2}, \lambda_{Z2}\}$ for Equations (15) in such forms as

$$\begin{cases} \lambda_{Yi} \left\{ \boldsymbol{Y}_{\boldsymbol{q}i}^{\mathrm{T}} \boldsymbol{q}_i + \boldsymbol{Y}_{\boldsymbol{x}i}^{\mathrm{T}} \dot{\boldsymbol{x}} + Y_{\varphi i}\dot{\varphi} + Y_{\psi i}\dot{\psi} + Y_{\theta i}\dot{\theta} \right\} = 0 \\ \lambda_{Zi} \left\{ \boldsymbol{Z}_{\boldsymbol{q}i}^{\mathrm{T}} \boldsymbol{q}_i + \boldsymbol{Z}_{\boldsymbol{x}i}^{\mathrm{T}} \dot{\boldsymbol{x}} + Z_{\varphi i}\dot{\varphi} + Z_{\psi i}\dot{\psi} + Z_{\theta i}\dot{\theta} \right\} = 0 \\ \qquad\qquad\qquad\qquad\qquad\qquad i = 1, 2 \end{cases} \tag{16}$$

where

$$\begin{cases} \boldsymbol{Y}_{\boldsymbol{q}i} = \frac{\partial Y_i}{\partial \boldsymbol{q}_i} - (r_i - \Delta x_i) \left\{ (-1)^i r_{Zz} \boldsymbol{e}_{iz} + r_{Zx} \boldsymbol{e}_{ix} \right. \\ \left. + \boldsymbol{r}_{Z21}^{\mathrm{T}} \boldsymbol{r}_Z \boldsymbol{e}_{iZ21} \right\} \\ \boldsymbol{Y}_{\boldsymbol{x}i} = \frac{\partial Y_i}{\partial \boldsymbol{x}}, \ Y_{\varphi i} = \frac{\partial Y_i}{\partial \varphi}, \ Y_{\psi i} = \frac{\partial Y_i}{\partial \psi} \\ Y_{\theta i} = \frac{\partial Y_i}{\partial \theta} + (-1)^i (r_i - \Delta x_i), \ i = 1, 2 \end{cases}$$

and

$$\begin{cases} \boldsymbol{Z}_{\boldsymbol{q}i} = \frac{\partial Z_i}{\partial \boldsymbol{q}_i} - (r_i - \Delta x_i) \left\{ (-1)^i r_{Yz} \boldsymbol{e}_{iz} + r_{Yx} \boldsymbol{e}_{ix} \right. \\ \left. + \boldsymbol{r}_{Z21}^{\mathrm{T}} \boldsymbol{r}_Y \boldsymbol{e}_{i2} \right\} \\ \boldsymbol{Z}_{\boldsymbol{x}i} = \frac{\partial Z_i}{\partial \boldsymbol{x}}, \ Z_{\varphi i} = \frac{\partial Z_i}{\partial \varphi}, \\ Z_{\psi i} = \frac{\partial Z_i}{\partial \psi} - (-1)^i (r_i - \Delta x_i), \ Z_{\theta i} = \frac{\partial Z_i}{\partial \theta}, i = 1, 2 \end{cases}$$

and $\boldsymbol{q}_1 = (q_{11}, q_{12}, q_{13})^{\mathrm{T}}$, $\boldsymbol{q}_2 = (q_{21x}, q_{21z}, q_{22})^{\mathrm{T}}$, $\boldsymbol{e}_{1z} = (1, 1, 1)^{\mathrm{T}}$, $\boldsymbol{e}_{2z} = (0, 1, 0)^{\mathrm{T}}$, $\boldsymbol{e}_{1x} = \boldsymbol{0}_3$, $\boldsymbol{e}_{2x} = (1, 0, 0)^{\mathrm{T}}$, $\boldsymbol{e}_{12} = \boldsymbol{0}_3$, and $\boldsymbol{e}_{22} = (0, 0, 1)$. To simplify notations, we rewrite Equation (16) into

$$\begin{cases} \lambda_{Yi} \boldsymbol{Y}_i^{\mathrm{T}} (\mathrm{d}\boldsymbol{X}/\mathrm{d}t) = 0 \\ \lambda_{Zi} \boldsymbol{Z}_i^{\mathrm{T}} (\mathrm{d}\boldsymbol{X}/\mathrm{d}t) = 0 \end{cases}, \ i = 1, 2 \tag{17}$$

where $\boldsymbol{X} = (\boldsymbol{q}_1^{\mathrm{T}}, \boldsymbol{q}_2^{\mathrm{T}}, \boldsymbol{x}^{\mathrm{T}}, \varphi, \phi, \theta)^{\mathrm{T}}$,

$$\begin{cases} \boldsymbol{Y}_1 = \left(\boldsymbol{Y}_{\boldsymbol{q}1}^{\mathrm{T}}, 0_2, \boldsymbol{Y}_{\boldsymbol{x}1}^{\mathrm{T}}, Y_{\varphi 1}, Y_{\phi 1}, Y_{\theta 1} \right)^{\mathrm{T}} \\ \boldsymbol{Y}_2 = \left(0, \boldsymbol{Y}_{\boldsymbol{q}2}^{\mathrm{T}}, \boldsymbol{Y}_{\boldsymbol{x}2}^{\mathrm{T}}, Y_{\varphi 2}, Y_{\phi 2}, Y_{\theta 2} \right)^{\mathrm{T}} \end{cases} \tag{18}$$

and

$$\begin{cases} \boldsymbol{Z}_1 = \left(\boldsymbol{Z}_{\boldsymbol{q}1}^{\mathrm{T}}, 0_2, \boldsymbol{Z}_{\boldsymbol{x}1}^{\mathrm{T}}, Z_{\varphi 1}, Z_{\phi 1}, Z_{\theta 1}\right)^{\mathrm{T}} \\ \boldsymbol{Z}_2 = \left(0, \boldsymbol{Z}_{\boldsymbol{q}2}^{\mathrm{T}}, \boldsymbol{Z}_{\boldsymbol{x}2}^{\mathrm{T}}, Z_{\varphi 2}, Z_{\phi 2}, Z_{\theta 2}\right)^{\mathrm{T}} \end{cases} \tag{19}$$

The reproducing force due to finger-tip deformation can be described as (see [13])

$$f_i(\Delta x_i, \Delta \dot{x}_i) = \bar{f}_i(\Delta x_i) + \xi_i(\Delta x_i)\Delta \dot{x}_i \tag{20}$$

where

$$\bar{f}_i(\Delta x_i) = k_i \Delta x_i^2,\ i = 1, 2 \tag{21}$$

with stiffness parameter $k_i > 0[\mathrm{N/m^2}]$ and $\xi_i(\Delta x_i)$ is a positive scalar function of Δx_i.

The viscosities around $\boldsymbol{r}_X$ at two contact points due to spinning motion around the opposing axis is represented by the following Rayleigh's dissipation functions:

$$R_{t1} = \frac{c_{t1}}{2} \parallel \{\boldsymbol{\omega} - (\dot{q}_{11} + \dot{q}_{12} + \dot{q}_{13})\boldsymbol{e}_z\}^{\mathrm{T}} \boldsymbol{r}_X \parallel^2 \tag{22}$$

$$R_{t2} = \frac{c_{t2}}{2} \parallel (\boldsymbol{\omega} - \dot{q}_{21z}\boldsymbol{e}_z - \dot{q}_{21x}\boldsymbol{e}_x - \dot{\boldsymbol{q}}_{22})^{\mathrm{T}} \boldsymbol{r}_X \parallel^2 \tag{23}$$

$$R_t = R_{t1} + R_{t2} \tag{24}$$

where R_{t1} expresses the Rayleigh's dissipation function at the left contact point, R_{t2} at the right contact point, both c_{t1} and c_{t2} positive constant values, $\boldsymbol{e}_x = (1, 0, 0)^{\mathrm{T}}$, and $\boldsymbol{e}_z = (0, 0, 1)^{\mathrm{T}}$. The function R_t is derived from taking into considerations that the difference between the rotational velocity of motion of the robot fingers and the rotational velocity of motion of the object relative to the $\boldsymbol{r}_X$ vector generates viscosity, and no viscosity arises in the case of equal velocities between the velocity of each robot finger and the velocity of the object relative to the $\boldsymbol{r}_X$ vector.

The Lagrangian for the overall fingers-object system can be expressed by the scalar quantity $L = K - P$, where K denotes the total kinetic energy expressed as

$$\begin{aligned} K = & \frac{1}{2}\dot{\boldsymbol{q}}_1^{\mathrm{T}} H_1 \dot{\boldsymbol{q}}_1 + \frac{1}{2} m_{21} \dot{\boldsymbol{x}}_{m21}^{\mathrm{T}} \dot{\boldsymbol{x}}_{m21} + \frac{1}{2}\dot{\boldsymbol{q}}_{21}^{\mathrm{T}} \bar{H}_{21} \dot{\boldsymbol{q}}_{21} \\ & + \frac{1}{2} m_{22} \dot{\boldsymbol{x}}_{m22}^{\mathrm{T}} \dot{\boldsymbol{x}}_{m22} \\ & + \frac{1}{2} \left(\dot{\boldsymbol{q}}_{21} + \dot{\boldsymbol{q}}_{22}\right)^{\mathrm{T}} \bar{H}_{22} \left(\dot{\boldsymbol{q}}_{21} + \dot{\boldsymbol{q}}_{22}\right) \\ & + \frac{1}{2} M \left(\dot{x}^2 + \dot{y}^2 + \dot{z}^2\right) + \frac{1}{2}\boldsymbol{\omega}^{\mathrm{T}} H_0 \boldsymbol{\omega} \end{aligned} \tag{25}$$

and P denotes the total potential energy expressed as

$$P = P_1 + P_2 - Mgy + \sum_{i=1,2} P_{\Delta xi} \tag{26}$$

where H_1 stands for the inertia matrix for finger 1, m_{21} the mass of the first link of the finger 2, m_{22} the mass of the second link of it, M the mass of the object, P_i the potential energy of finger i, g the gravity constant, and $P_{\Delta xi} (= \int_0^{\Delta x_i} \bar{f}_i(\xi)\mathrm{d}\xi)$ the potential energy of reproducing force for finger i, and H_0 is given in the following:

$$H_0 = R(t) H R^{\mathrm{T}}(t) \tag{27}$$

where H stands for the constant inertia matrix of the object that must be evaluated on the basis of fixed body coordinates $O_{\mathrm{c.m.}}$-XYZ, that is,

$$H = \begin{pmatrix} I_{XX} & I_{XY} & I_{XZ} \\ I_{YX} & I_{YY} & I_{YZ} \\ I_{ZX} & I_{ZY} & I_{ZZ} \end{pmatrix} \tag{28}$$

Similarly, $H_{2i} (i = 1, 2)$ is given in the following:

$$H_{2i} = R_{2i}(t) \bar{H}_{2i} R_{2i}^{\mathrm{T}}(t) \tag{29}$$

where $\bar{H}_{21}$ similarly stands for the constant inertia matrix of the first link of the robot finger 2 and $\bar{H}_{22}$ the constant inertia matrix of its second link, that must be expressed on the basis of fixed robot link coordinates $O_{\mathrm{c.m.}2i}$-$X_{2i}Y_{2i}Z_{2i}$ respectively, that is,

$$\bar{H}_{2i} = \begin{pmatrix} I_{XX2i} & I_{XY2i} & I_{XZ2i} \\ I_{YX2i} & I_{YY2i} & I_{YZ2i} \\ I_{ZX2i} & I_{ZY2i} & I_{ZZ2i} \end{pmatrix}, \quad i = 1, 2 \tag{30}$$

where

$$R_{22}(t) = (\boldsymbol{r}_{X22}, \boldsymbol{r}_{Y22}, \boldsymbol{r}_{Z22}) \in SO(3) \tag{31}$$

Thus, owing to the variational principle applied to the form

$$\begin{aligned} -\int_{t_0}^{t_1} \delta L \mathrm{d}t = & \int_{t_0}^{t_1} \sum_{i=1,2} \Big\{ \boldsymbol{u}_i^{\mathrm{T}} \delta \boldsymbol{q}_i \\ & - \left(\lambda_{Yi} \boldsymbol{Y}_i^{\mathrm{T}} + \lambda_{Zi} \boldsymbol{Z}_i^{\mathrm{T}}\right) \delta \boldsymbol{X} \Big\} \mathrm{d}t \\ & - \int_{t_0}^{t_1} \Big\{ \frac{\partial R_t}{\partial \dot{\boldsymbol{X}}^{\mathrm{T}}} \delta \boldsymbol{X} + \sum_{i=1,2} \xi_i(\Delta x_i) \Delta \dot{x}_i \frac{\partial \Delta \dot{x}_i}{\partial \dot{\boldsymbol{X}}^{\mathrm{T}}} \delta \boldsymbol{X} \Big\} \mathrm{d}t \end{aligned} \tag{32}$$

we obtain a set of Lagrange's equations of motion of the overall system:

$$\begin{aligned} & H_i \ddot{\boldsymbol{q}}_i + \left\{ \frac{1}{2}\dot{H}_i + S_i \right\} \dot{\boldsymbol{q}}_i + \frac{\partial R_t}{\partial \dot{\boldsymbol{q}}_i} - (-1)^i f_i J_{0i}^{\mathrm{T}} \boldsymbol{r}_X \\ & \quad - \lambda_{Yi} \boldsymbol{Y}_{\boldsymbol{q}i} - \lambda_{Zi} \boldsymbol{Z}_{\boldsymbol{q}i} + \boldsymbol{g}_i = \boldsymbol{u}_i, \qquad i = 1, 2 \end{aligned} \tag{33}$$

$$\begin{aligned} & M\ddot{\boldsymbol{x}} - (f_1 - f_2)\boldsymbol{r}_X + (\lambda_{Y1} + \lambda_{Y2})\boldsymbol{r}_Y \\ & \quad + (\lambda_{Z1} + \lambda_{Z2})\boldsymbol{r}_Z - Mg \begin{pmatrix} 0 \\ 1 \\ 0 \end{pmatrix} = 0 \end{aligned} \tag{34}$$

$$\begin{aligned} & H_0 \dot{\boldsymbol{\omega}} + \left(\frac{1}{2}\dot{H}_0 + S\right)\boldsymbol{\omega} + \frac{\partial R_t}{\partial \boldsymbol{\omega}} + f_1 \begin{pmatrix} 0 \\ -Z_1 \\ Y_1 \end{pmatrix} \\ & \quad + f_2 \begin{pmatrix} 0 \\ Z_2 \\ -Y_2 \end{pmatrix} - \lambda_{Y1} \begin{pmatrix} Z_1 \\ 0 \\ l_1 \end{pmatrix} - \lambda_{Y2} \begin{pmatrix} Z_2 \\ 0 \\ -l_2 \end{pmatrix} \\ & \quad - \lambda_{Z1} \begin{pmatrix} -Y_1 \\ -l_1 \\ 0 \end{pmatrix} - \lambda_{Z2} \begin{pmatrix} -Y_2 \\ l_2 \\ 0 \end{pmatrix} = 0 \end{aligned} \tag{35}$$

where calculation of partial differentiations of Y_i, Z_i in φ, ψ, θ is presented in Table I. Further, it is possible to see

TABLE I

PARTIAL DERIVATIVES OF CONSTRAINTS IN (φ, ψ, θ).

$\frac{\partial P_{\Delta x1}}{\partial \varphi} = \frac{\partial P_{\Delta x2}}{\partial \varphi} = 0$
$\frac{\partial Y_i}{\partial \varphi} = (x_{0i} - x)^{\mathrm{T}} \frac{\partial r_Y}{\partial \varphi} = (x_{0i} - x)^{\mathrm{T}} r_Z = Z_i$
$\frac{\partial Y_i}{\partial \psi} = (x_{0i} - x)^{\mathrm{T}} \frac{\partial r_Y}{\partial \psi} = 0$
$\frac{\partial Y_i}{\partial \theta} = (x_{0i} - x)^{\mathrm{T}} \frac{\partial r_Y}{\partial \theta} = -(x_{0i} - x)^{\mathrm{T}} x_X = -(-1)^i (r_i - \Delta x_i + l_i)$
$\frac{\partial Z_i}{\partial \varphi} = (x_{0i} - x)^{\mathrm{T}} \frac{\partial r_Z}{\partial \varphi} = (x_{0i} - x)^{\mathrm{T}} r_Y = -Y_i$
$\frac{\partial Z_i}{\partial \psi} = (x_{0i} - x)^{\mathrm{T}} \frac{\partial r_Z}{\partial \psi} = -(x_{0i} - x)^{\mathrm{T}} r_X = (-1)^i (r_i - \Delta x_i + l_i)$
$\frac{\partial Z_i}{\partial \theta} = (x_{0i} - x)^{\mathrm{T}} \frac{\partial r_Z}{\partial \theta} = 0$
$Y_{\varphi i} = \frac{\partial Y_i}{\partial \varphi} = Z_i,\ Z_{\varphi i} = \frac{\partial Z_i}{\partial \varphi} = -Y_i$
$Y_{\psi i} = \frac{\partial Y_i}{\partial \psi} = 0,\ Z_{\psi i} = \frac{\partial Z_i}{\partial \psi} - (-1)^i (r_i - \Delta x_i) = (-1)^i l_i$
$Y_{\theta i} = \frac{\partial Y_i}{\partial \theta} + (-1)^i (r_i - \Delta x_i) = -(-1)^i l_i,\ Z_{\theta i} = 0$

from $P_{\Delta xi} (i = 1, 2)$ and Equations (12) and (13) that

$$\begin{cases} \frac{\partial (P_{\Delta x1} + P_{\Delta x2})}{\partial \boldsymbol{q}_i} = -(-1)^i f_i J_i^{\mathrm{T}} \boldsymbol{r}_X,\ i = 1, 2 \\ \frac{\partial (P_{\Delta x1} + P_{\Delta x2})}{\partial \boldsymbol{x}} = -(f_1 - f_2)\, \boldsymbol{r}_X \\ \frac{\partial (P_{\Delta x1} + P_{\Delta x2})}{\partial \varphi} = 0,\ \ \frac{\partial (P_{\Delta x1} + P_{\Delta x2})}{\partial \psi} = -f_1 Z_1 + f_2 Z_2 \\ \frac{\partial (P_{\Delta x1} + P_{\Delta x2})}{\partial \theta} = f_1 Y_1 - f_2 Y_2 \end{cases} \tag{36}$$

$$\begin{cases} \boldsymbol{Y}_{\boldsymbol{x}i} = \partial Y_i / \partial \boldsymbol{x} = -\boldsymbol{r}_Y \\ \boldsymbol{Z}_{\boldsymbol{x}i} = \partial Z_i / \partial \boldsymbol{x} = -\boldsymbol{r}_Z \end{cases} \tag{37}$$

From taking inner products between $\dot{\boldsymbol{q}}_i$ and Equation (33), $\dot{\boldsymbol{x}}$ and Equation (34), and $\boldsymbol{\omega}$ and Equation (35), we obtain the relation

$$\sum_{i=1,2} \dot{\boldsymbol{q}}_i^{\mathrm{T}} \boldsymbol{u}_i = \frac{\mathrm{d}}{\mathrm{d}t} (K + P) + 2R_t + \sum_{i=1,2} \xi(\Delta x_i) \Delta \dot{x}_i^2 \tag{38}$$

Finally, we interestingly notice six wrench vectors composed of accompaniments to f_1, f_2, λ_{Y1}, λ_{Y2}, λ_{Z1}, and λ_{Z2} in Equations (34) and (35). The six wrench vectors and the external force composed of the last term in Equation (34) work on the 3-dimensional object.

IV. CONTROL SIGNALS

A control input realizing stable grasping under the gravity effect without using object kinematics or external sensing, which is called "blind grasping", is proposed as follows:

$$\begin{aligned} \boldsymbol{u}_i = & -C_i \dot{\boldsymbol{q}}_i + (-1)^i \frac{f_d}{r_1 + r_2} J_{0i}^{\mathrm{T}} (\boldsymbol{x}_{01} - \boldsymbol{x}_{02}) \\ & - \frac{\hat{M} g}{2} \frac{\partial y_{0i}}{\partial \boldsymbol{q}_i} - r_i \hat{N}_{iz} \boldsymbol{e}_{iz} \\ & - r_i \hat{N}_{ix} \boldsymbol{e}_{ix} - r_i \hat{N}_{i2} \boldsymbol{e}_{i2}, \quad i = 1, 2 \end{aligned} \tag{39}$$

where

$$\begin{aligned} \hat{M} = & \hat{M}(0) + \int_0^t \frac{g \gamma_M^{-1}}{2} \sum_{i=1,2} \left(\frac{\partial y_{0i}}{\partial \boldsymbol{q}_i} \right)^{\mathrm{T}} \boldsymbol{q}_i \mathrm{d}\tau \\ = & \hat{M}(0) + \frac{g \gamma_M^{-1}}{2} (y_{01}(t) + y_{02}(t) \\ & - y_{01}(0) - y_{02}(0)) \end{aligned} \tag{40}$$

$$\begin{aligned} \hat{N}_{1z} = & \gamma_{N1z}^{-1} \int_0^t \left(r_1 \boldsymbol{e}_{1z}^{\mathrm{T}} \dot{\boldsymbol{q}}_1 \right) \mathrm{d}\tau \\ = & r_{N1z}^{-1} r_i \boldsymbol{e}_{1z}^{\mathrm{T}} \left(\boldsymbol{q}_1(t) - \boldsymbol{q}_1(0) \right) \end{aligned} \tag{42}$$

$$\begin{aligned} \hat{N}_{2z} = & \gamma_{N2z}^{-1} \int_0^t \left(r_2 \boldsymbol{e}_{2z}^{\mathrm{T}} \dot{\boldsymbol{q}}_2 \right) \mathrm{d}\tau \\ \hat{N}_{2x} = & \gamma_{N02}^{-1} \int_0^t \left(r_i \dot{q}_{21x} \right) \mathrm{d}\tau \\ \hat{N}_{22} = & \gamma_{N22}^{-1} \int_0^t \left(r_2 \dot{q}_{22} \right) \mathrm{d}\tau \\ = & \gamma_{N22}^{-1} r_2 \left(q_{22}(t) - q_{22}(0) \right) \end{aligned} \tag{43}$$

and γ_M, $\gamma_{Niz} (i = 1, 2)$, γ_{N2x}, and γ_{N22} are positive constants. The form is nothing but the control signal proposed in the rigid contact case [11] [13]. The third term of the right hand side of Equation (41) is a signal based upon the opposable force between O_{01} and O_{02} (not between O_1 and O_2, because positions of O_1 and O_2 can not be measured). The fourth term stands for compensation for the object mass based upon its estimator. The fifth term is introduced for saving excess movements of finger joints from the initial pose. Next define

$$f_0 = f_d \left(1 + \frac{l_1 + l_2 - \Delta x_1 - \Delta x_2}{r_1 + r_2} \right) \tag{44}$$

Differently from the case of rigid finger-ends [11], f_0 is not a constant but dependent on the magnitude of $\Delta x_1 + \Delta x_2$. Nevertheless, it is possible to find $\Delta x_{di} (i = 1, 2)$ for a given $f_d > 0$ so that they satisfy

$$\bar{f}_i(\Delta x_{di}) = \left(1 + \frac{l_1 + l_2 - \Delta x_{d1} - \Delta x_{d2}}{r_1 + r_2} \right) f_d,\ i = 1, 2 \tag{45}$$

because $\bar{f}_i(\Delta x)$ is of the form of $\bar{f}_i(\Delta x) = k_i \Delta x^2$(Equation (21)). Substituting this control signals (Equation (39)) into Equations (33), (34), and (35) yields

$$\begin{aligned} & H_i \ddot{\boldsymbol{q}}_i + \left\{ \frac{1}{2} \dot{H}_i + S_i + C_i \right\} \dot{\boldsymbol{q}}_i + \frac{\partial R_t}{\partial \dot{\boldsymbol{q}}_i} - (-1)^i J_{0i}^{\mathrm{T}} \Delta f_i \boldsymbol{r}_X \\ & - \Delta \lambda_{Yi} \boldsymbol{Y}_{\boldsymbol{q}i} - \Delta \lambda_{Zi} \boldsymbol{Z}_{\boldsymbol{q}i} + \frac{\Delta M g}{2} \left(\frac{\partial y_{0i}}{\partial \boldsymbol{q}_i} \right) + r_i \Delta N_{iz} \boldsymbol{e}_{iz} \\ & + r_i \Delta N_{ix} \boldsymbol{e}_{ix} + r_i \Delta N_{i2} \boldsymbol{e}_{i2} + \boldsymbol{g} = 0, \quad i = 1, 2 \end{aligned} \tag{46}$$

$$\begin{aligned} & M \ddot{\boldsymbol{x}} - (\Delta f_1 - \Delta f_2) \boldsymbol{r}_X + (\Delta \lambda_{Y1} + \Delta \lambda_{Y2}) \boldsymbol{r}_Y \\ & + (\Delta \lambda_{Z1} + \Delta \lambda_{Z2}) \boldsymbol{r}_Z = 0 \end{aligned} \tag{47}$$

$$\begin{aligned} & H_0 \dot{\boldsymbol{\omega}} + \left(\frac{1}{2} \dot{H}_0 + S \right) \boldsymbol{\omega} + \frac{\partial R_t}{\partial \boldsymbol{\omega}} + \Delta f_1 \begin{pmatrix} 0 \\ -Z_1 \\ Y_1 \end{pmatrix} \\ & + \Delta f_2 \begin{pmatrix} 0 \\ Z_2 \\ -Y_2 \end{pmatrix} - \Delta \lambda_{Y1} \begin{pmatrix} Z_1 \\ 0 \\ l_1 \end{pmatrix} - \Delta \lambda_{Y2} \begin{pmatrix} Z_2 \\ 0 \\ -l_2 \end{pmatrix} \\ & - \Delta \lambda_{Z1} \begin{pmatrix} -Y_1 \\ -l_1 \\ 0 \end{pmatrix} - \Delta \lambda_{Z2} \begin{pmatrix} -Y_2 \\ l_2 \\ 0 \end{pmatrix} - \begin{pmatrix} S_x \\ S_y \\ S_z \end{pmatrix} = 0 \end{aligned} \tag{48}$$

where

$$\Delta f_i = \bar{f}_i - f_0 - (-1)^i \frac{Mg}{2} r_{Xy} \tag{49}$$

$$\Delta\lambda_{Yi} = \lambda_{Yi} + (-1)^i \frac{f_d}{r_1 + r_2}(Y_1 - Y_2) - \frac{Mg}{2} r_{Yy} \tag{50}$$

$$\Delta\lambda_{Zi} = \lambda_{Zi} + (-1)^i \frac{f_d}{r_1 + r_2}(Z_1 - Z_2) - \frac{Mg}{2} r_{Zy} \tag{51}$$

$$\begin{cases} \Delta M = \hat{M} - M,\ \Delta N_{iz} = \hat{N}_{iz} - N_{iz},\ i = 1, 2 \\ \Delta N_{2x} = \hat{N}_{2x} - N_{x2},\ \Delta N_{22} = \hat{N}_{22} - N_{22} \end{cases} \tag{52}$$

$$\begin{aligned} N_{iz} = & \frac{f_d}{r_1 + r_2} \frac{(r_i - \Delta x_i)}{r_i} \Big\{ (Y_1 - Y_2) r_{Zz} \\ & - (Z_1 - Z_2) r_{Yz} \Big\} \\ & - (-1)^i \frac{(r_i - \Delta x_i)}{r_i} \frac{Mg}{2} \Big\{ r_{Yy} r_{Zz} \\ & - r_{Zy} r_{Yz} \Big\},\ i = 1, 2 \end{aligned} \tag{53}$$

$$\begin{aligned} N_{2x} = & \frac{f_d}{r_1 + r_2} \frac{(r_2 - \Delta x_2)}{r_2} \Big\{ (Y_1 - Y_2) r_{Zx} \\ & - (Z_1 - Z_2) r_{Yx} \Big\} \\ & - \frac{(r_2 - \Delta x_i)}{r_2} \frac{Mg}{2} \Big\{ r_{Yy} r_{Zx} \\ & - r_{Zy} r_{Yx} \Big\} \end{aligned} \tag{54}$$

$$\begin{aligned} N_{22} = & \frac{f_d}{r_1 + r_2} \frac{(r_2 - \Delta x_2)}{r_2} \Big\{ (Y_1 - Y_2) \boldsymbol{r}_{Z21}^{\mathrm{T}} \boldsymbol{r}_Z \\ & - (Z_1 - Z_2) \boldsymbol{r}_{Z21}^{\mathrm{T}} \boldsymbol{r}_Y \Big\} \\ & - \frac{(r_2 - \Delta x_i)}{r_2} \frac{Mg}{2} \Big\{ \boldsymbol{r}_{Z21}^{\mathrm{T}} \boldsymbol{r}_Z r_{Yy} \\ & - \boldsymbol{r}_{Z21}^{\mathrm{T}} \boldsymbol{r}_Y r_{Zy} \Big\} \end{aligned} \tag{55}$$

$$S_x = \frac{Mg}{2} \{ (Z_1 + Z_2) r_{Yy} - (Y_1 + Y_2) r_{Zy} \} \tag{56}$$

$$\begin{aligned} S_y = & \frac{f_d}{r_1 + r_2} (r_1 - \Delta x_1 + r_2 - \Delta x_2)(Z_1 - Z_2) \\ & - \frac{Mg}{2} \{ r_{Xy}(Z_1 + Z_2) + r_{Zy}(l_1 - l_2) \} \end{aligned} \tag{57}$$

$$\begin{aligned} S_z = & - \frac{f_d}{r_1 + r_2} (r_1 - \Delta x_1 + r_2 - \Delta x_2)(Y_1 - Y_2) \\ & + \frac{Mg}{2} \{ r_{Xy}(Y_1 + Y_2) + r_{Yy}(l_1 - l_2) \} \end{aligned} \tag{58}$$

V. Numerical Simulation Results and Initial Values

We carry out numerical simulations based on the physical parameters of the fingers-object system given in Table II and the parameters of control gains given in Table III in order to confirm the stability of motion of the overall dynamics applied by the proposed control input. It is noted that δq_{21x} and δq_{21z} have a meaning as a virtual displacement but quantity of δq_{21x} and δq_{21z} do not have physical meanings of rotational angels. Hence we set the virtual angles $q_{21x}(0)$ and $q_{21z}(0)$ to zero respectively as shown Table III and the virtual angles do not directly affect numerical simulations at all. The results of numerical simulations, representing key variables of fingers-object system, converge to some constant values as shown in Fig.7. It is confirmed that spinning motion arises but eventually it ceases after 10 seconds, that is, $\boldsymbol{\omega} \to 0$ as $t \to \infty$ seen through Figs.6 and 7. On the other hand, if we set the damping parameters c_{t1} and c_{t2} to zero respectively, we can see that spinning motion continues eternally. Therefore it is confirmed that motion of the overall fingers-object system is stabilized from the viewpoint of simulations.

TABLE II

Physical parameters of the fingers and object.

$l_{11} = l_{12} = l_{22}$	length	0.040 [m]
l_{13}	length	0.030 [m]
l_{21}	length	0.060 [m]
m_{11}	weight	0.043 [kg]
m_{12}	weight	0.031 [kg]
m_{13}	weight	0.020 [kg]
m_{21}	weight	0.060 [kg]
m_{22}	weight	0.040 [kg]
r_0	link radius	0.005 [m]
$r_i (i = 1, 2)$	radius	0.010 [m]
L	base length	0.063 [m]
M	object weight	0.040 [kg]
$l_i (i = 1, 2)$	object width	0.015 [m]
h	object height	0.050 [m]
$k_i (i = 1, 2)$	stiffness	3.000×10^5[N/m^2]
$c_{\Delta i} (i = 1, 2)$	viscosity	1000.0[Ns/m^2]
$c_{t1} = c_{t2}$	viscosity	5.0×10^{-4} [Nms]

TABLE III

Parameters of control signals.

f_d	internal force	1.000 [N]
c	damping coefficient	0.001 [Nms]
γ_M	regressor gain	0.050 [m^2/kgs^2]
$\gamma_{Niz} (i = 1, 2)$	regressor gain	5.000×10^{-4} [s^2/kg]
γ_{N2x}	regressor gain	5.000×10^{-4} [s^2/kg]
γ_{N22}	regressor gain	5.000×10^{-4} [s^2/kg]
$\hat{M}(0)$	initial estimate value	0.020 [kg]
$\hat{N}_{iz}(0) (i = 1, 2)$	initial estimate value	0.000 [N]
$\hat{N}_{2x}(0)$	initial estimate value	0.000 [N]
$\hat{N}_{22}(0)$	initial estimate value	0.000 [N]
$q_{21x}(0) = q_{21z}(0)$	initial virtual angle	0.000[deg]

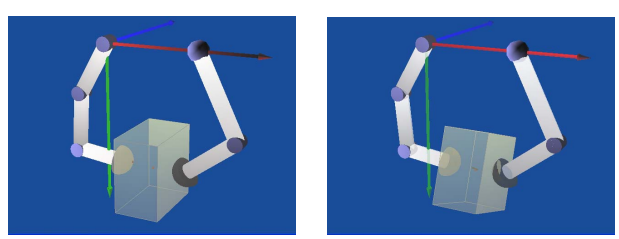

(a) Initial pose (b) After 10 seconds

Fig. 6. Motions of pinching a 3-D object under the gravity effect

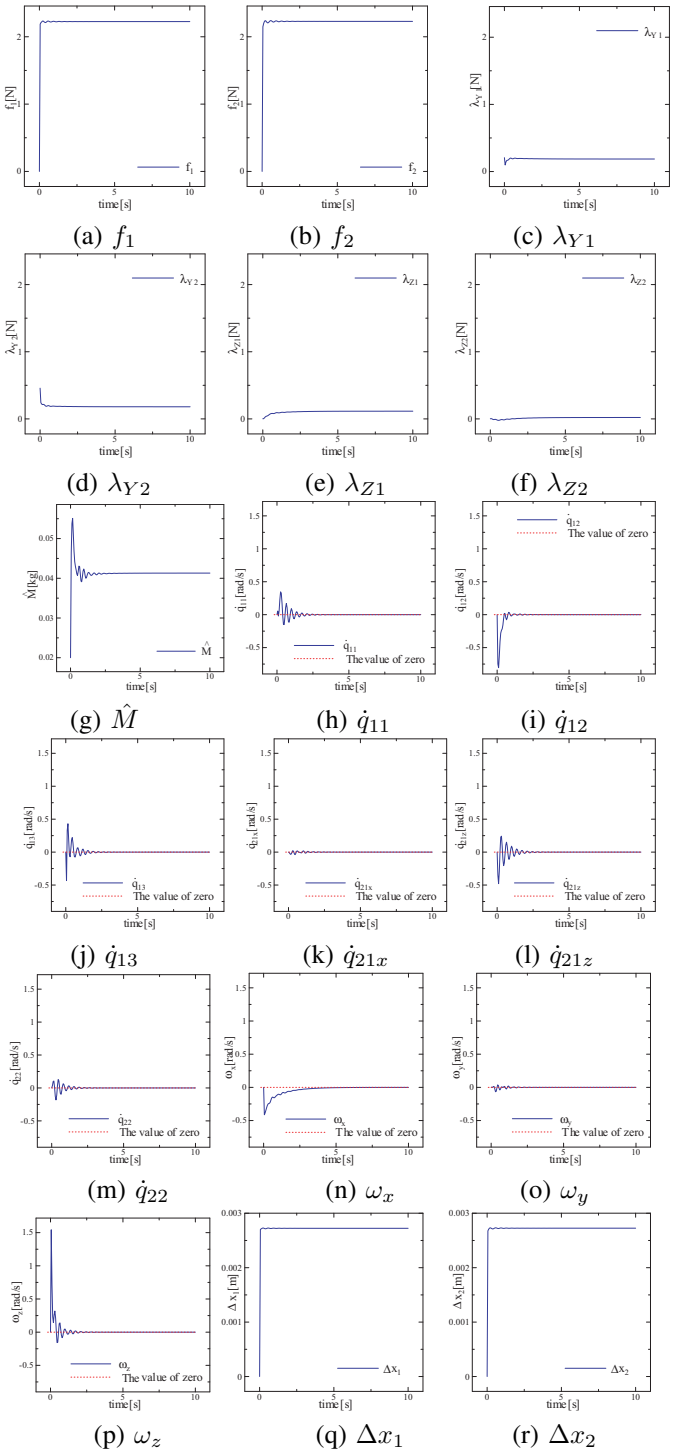

(a) f_1 (b) f_2 (c) λ_{Y1}

(d) λ_{Y2} (e) λ_{Z1} (f) λ_{Z2}

(g) $\hat{M}$ (h) $\dot{q}_{11}$ (i) $\dot{q}_{12}$

(j) $\dot{q}_{13}$ (k) $\dot{q}_{21x}$ (l) $\dot{q}_{21z}$

(m) $\dot{q}_{22}$ (n) ω_x (o) ω_y

(p) ω_z (q) Δx_1 (r) Δx_2

Fig. 7. Transient responses of physical variables

VI. Conclusion

A saddle joint model with orderless actuations and rolling constraints have been treated in a faithful manner and incorporated into the overall fingers-object system. It is shown that 3-D pinching by two robot fingers, one is a 3-DOFs planar finger (resembles the index finger) and the other is a 3-DOFs finger with a saddle joint (the thumb), is performed numerically by using the derived computational model. Differently from the previous paper [10], the overall fingers-object dynamics are derived as a full-variables model. It is shown through computer simulations that spinning motion between finger tips and the object arises but eventually stops by virtue of the incorporated viscosity model exerted on rotational motion of the object around $\boldsymbol{r}_X$ vector at two contact points between a left or right finger tip and the object surface. Numerical simulation results showed the stability of motion of the overall fingers-object dynamics to which the proposed control input is applied. However, to confirm the effectiveness of our proposed control input in a sound meaning, the analysis of its stability is indispensable and should be carried out from the mathematically reasonable viewpoint. Finally it is shown that the proposed viscosity model plays a crucial role in pinching a 3-D object.

VII. Acknowledgments

This work was partially supported by Japan Society for the Promotion of Science (JSPS), Grant-in-Aid for Scientific Research (B) (20360117).

References

[1] John Napier, *Hands*, Princeton Univ. Press, Princeton, NJ, USA,1993.
[2] R. M. Murray, Z. Li, and S. S. Sastry, *A Mathematical Introduction to Robotic Manipulation*, CRC Press, Boca Raton,FL, USA and Tokyo, Japan, 1994.
[3] M. R.Cutkosky, *Robotic Grasping and Fine Manipulation*, Kluwer Academic, Dordrecht, Netherlands, 1985.
[4] A. Bicchi, "Hands for dexterous manipulation and robust grasping: A difficult road toward simplicity," *IEEE Trans. on Robotics and Automation*, Vol.16, No. 6, pp.652–662, 2000.
[5] D.J. Montana, "The kinematics of contact and grasp", *Int. J.of Robotics Research*, Vol. 7, No. 3, pp.17-32, 1988.
[6] D.J. Montana, "Contact stability for two-fingered grasps", *IEEE Trans. on Robotics and Automation*, vol.8, no.4, pp.421-430,1992.
[7] A.A. Shabana, *Computational Dynamics, Second Edition*, Wiley-Interscience, New York, USA, 2001.
[8] S. Arimoto, P.T.A. Nguyen, H.-Y. Han, and Z. Doulgeri, "Dynamics and control of a set of dual fingers with soft tips", *Robotica*, vol.18, no.1, 2000, pp.71-80.
[9] S.Arimoto, K.Tahara, J.-H.Bae, M.Yoshida, "A stability theory of a manifold: concurrent realization of grasp and orientation control of an object by a pair of robot fingers", *Robotica*, Vol.21, No.2, pp.163-178, 2003.
[10] S.Arimoto, M.Yoshida, J.-H.Bae, "Modeling of 3-D object manipulation by multi-joint robot fingers under non-holonomic constraints and stable blind grasping", *JSME Journal of System Design and Dynamics*, Vol.1, No.3, pp.434-446, 2007.
[11] S. Arimoto and M. Yoshida, "Modeling and Control of Three-Dimensional Grasping by a Pair of Robot Fingers", *SICE J. of Control, Measurement, and System Integration*, Vol.1, No.1, pp.2-11, 2008.
[12] M. Yoshida, S. Arimoto, and Z. W. Luo, "Three-Dimensional Object Manipulation by Two Robot Fingers with Soft Tips and Minimum D.O.F", *Proc. of the 2008 IEEE Robotics and Automation*, Pasadena, CA, May 19-23,pp.4707-4714, 2008.
[13] S. Arimoto *Control Theory of Multi-fingered Hands*, Springer-Verlag, London, 2008.
[14] Gerard J. Tortora and Sandra R. Grabowski *Introduction to the human body:The essentials of anatomy & physiology*, Wiley, NJ, USA, 2004.